A DIGITAL COMPUTER PROPULSION CONTROL FACILITY - DESCRIPTION OF CAPABILITIES AND SUMMARY OF EXPERIMENTAL PROGRAM RESULTS

John R. Zeller, Dale J. Arpasi, and Bruce Lehtinen
NASA Lewis Research Center

SUMMARY

Flight-weight digital computers are being used today to carry out many of the propulsion system control functions previously delegated exclusively to hydromechanical controllers. An operational digital computer facility for propulsion control mode studies has been used successfully in several experimental programs at the Lewis Research Center. This paper describes the system and some of the results thus far obtained. These results are concerned with engine control, inlet control, and inlet-engine integrated control. Analytical designs for the digital propulsion control modes include both classical and modern/optimal techniques.

INTRODUCTION

With each advancement in integrated-circuit technology, the reliability of electronic digital computers designed for use in severe aircraft environments improves. As a result, flight-weight digital computers will be used to carry out more and more of the propulsion control functions now being handled by continuous hydromechanical controllers. Flight-weight digital computer controllers have already been selected for operational flight applications as a full-authority supersonic inlet control and as a supervisory control on an afterburning turbofan engine. In addition to operational flight applications, a general-purpose electronic digital computer controller can greatly simplify the development of control modes for advanced airbreathing propulsion systems. The many scheduling and logical manipulations necessary in the control of complex high-performance propulsion systems are well suited to the capabilities of a digital computer. Control modes can be easily implemented in software and checked out without actual flight hardware development.

Because of the benefits of a general-purpose digital computer for propulsion control mode development, the Lewis Research Center put into operation several years ago the

Digital Computer Propulsion Control Facility for developing advanced propulsion control modes. It is designed to permit real-time, on-line implementation of controls for various configurations of airbreathing propulsion systems operating in sea-level, altitude, and wind tunnel test facilities.

This paper describes the capabilities of this facility as they relate to the requirements of propulsion system control mode research and discusses various test programs in which this digital facility was used successfully. First, the Digital Computer Propulsion Control Facility in use at the Lewis Research Center is described in detail. Next, the various programs in which the facility was employed as an active control system are briefly described. The results obtained from the various programs are then summarized. These results include data related to such things as inlet shock-position control and engine fail-operational control. Finally, some of the present activities in this area are discussed and future areas of investigation for digital propulsion control recommended.

DIGITAL COMPUTER PROPULSION CONTROL FACILITY

Design Considerations

The Digital Computer Propulsion Control Facility was designed to provide versatile control of airbreathing propulsion systems including (1) inlet control, such as shock-position regulation and restart scheduling; (2) engine control to provide thrust and specific-fuel-consumption optimization under operational restrictions; and (3) combined inlet-engine interaction optimization.

The prime considerations in the design of the computer control facility were overall signal processing speed and computational capacity. The system must be capable of accepting the necessary system inputs, processing them, and outputting the commands within the frequency range of the propulsion system dynamics. For example, inlet control generally requires a high rate of control command updates but relatively few measurements and calculations. On the other hand, engine control does not generally require a high rate of control command updates but could entail the measurement of many engine parameters and could require extensive control computations.

System processing speed is a function of computer computational speed and the versatility of the input-output structure. Computational speed is maximized through the use of an efficient programming language and a fast-response-time computer. Computer response time is denoted by memory cycle time, which is the time it takes to read and restore a computer word in memory. Typical memory cycle times of real-time computers presently available range from a fraction of a microsecond to a few microseconds. Programming languages become less efficient as they are removed from the basic machine

language. The most efficient language offers a one-to-one correspondence with machine language. This language is generally called assembly language. The versatility of the assembly instruction set is of prime importance in the selection of a digital computer for purposes of control.

The input-output structure should require a minimum of machine computation time. Direct automatic transfer of blocks of data to and from computer memory on a cycle-stealing basis is necessary. This method causes disruption of the computation process for only one machine cycle per word of data transferred.

In addition to these internal equipment considerations, external characteristics of the digital control equipment were also a consideration. Control development is best done with the aid of comprehensive analog or hybrid simulations of the propulsion system. Since long-line communication between the Lewis simulation laboratory and all the planned propulsion test areas did not originally exist, portability of the digital control equipment was a requirement.

General Facility Description

The digital computer controller is made up of several distinct units:

(1) A digital computer designed for real-time control applications

(2) A digital interface capable of converting both analog and frequency signals to computer-compatible digital words and converting computer-generated words to analog and logical outputs

(3) Programming peripherals consisting of a high-speed, paper-tape reader and punch and a teletype

(4) A signal processing unit (SPU) which provides signal conditioning and monitoring, as well as some analog computation capability, between the digital interface and the propulsion system to be controlled

The digital computer, the digital interface, and the programming peripherals were supplied as a system from a digital computer manufacturer. The signal processing unit was assembled at Lewis from purchased components.

The system, excluding the teletype, is housed in five distinct racks (fig. 1) requiring approximately 3.4 running meters of floor space. Intercabinet cabling is accomplished in the rear and allows a maximum of 3.05 meters of spacing between adjacent cabinets. The system was designed to be portable. Typical teardown and setup time is 1 day, and complete system checkout requires 1 week

The block diagram of figure 2 illustrates the basic units and interconnection of the digital control system. All signals, to and from the propulsion system, pass through the signal processing unit (SPU).

The SPU will accept high level (±10 V range) analog signals already amplified and signal conditioned from standard pressure transducers and thermocouples. It will accept frequency signals directly from flowmeters and magnetic speed transducers. System outputs may be directed to proportional electrohydraulic servosystems or on-off types of devices. These serve as the control inputs to the propulsion system manipulated variables. The SPU was designed to increase flexibility in the calibration and operation of the control system. In particular, the SPU provides

(1) Ground isolation between the facility and the control unit
(2) Signal filtering
(3) Analog computation for propulsion system simulation or generation of time-dependent control functions
(4) Flexibility in signal routing between the facility and the control unit
(5) Calibration of the system
(6) Comparators and signal conditioners for use with priority interrupts
(7) Signal monitoring

Figure 3 illustrates the SPU cabinet layout and its equipment complement.

The digital interface consists of a high-level, analog signal acquisition unit; a frequency signal acquisition unit; an analog signal output unit; a logical output unit; and an external priority interrupt processor. The digital interface communicates with the computer on either a single-word or a block-data-transfer basis. The programming peripherals communicate only by single-character transfer. The signal-processing capability of the system is given in table I. Table II contains a complete list of specifications for the computer and digital interface equipment.

The computer itself is programmed through the use of paper tape. The system includes a high-speed, paper-tape reader and punch. The reader operates at 300 characters per second and punches at 110 characters per second. One character consists of eight binary bits. Paper tapes may be generated on an ASR 35 teletype and may also be read into the computer by this unit.

A more detailed description of the complete digital computer facility is given in reference 1.

Digital Propulsion Control Programs

The Digital Computer Propulsion Control Facility just described has been in operation at Lewis for approximately $4\frac{1}{2}$ years. The facility has been used continuously throughout that period. The experimental programs in which it has been utilized for propulsion control mode research are summarized as follows:

(1) Mixed-compression experimental inlet in the 10- by 10-Foot Supersonic Wind Tunnel: High-performance shock-position and restart control studies using both

classical and modern control design techniques

(2) Full-authority digital computer control of a turbojet engine in a sea-level test stand: Bill-of-material control modes with prediction techniques

(3) Full-scale symmetric, mixed-compression inlet in the 10- by 10-Foot Supersonic Wind Tunnel: Digital implementation of bill-of-material control modes as well as research control modes

(4) Fail-operational type of turbojet engine controller: Evaluation in sea-level test stand

(5) Integrated engine-inlet control: Mixed-compression inlet and afterburning turbofan engine in the 10- by 10-Foot Supersonic Wind Tunnel

In each of these experimental programs, the software implementations of the digital propulsion control laws were checked out and debugged with real-time analog simulations of the inlet and/or engine. This activity was carried out with the computer equipment located in the simulation laboratory. In the early experimental programs, the equipment would then be physically moved to the control rooms of the experimental facilities. The most recent programs, though, have employed a central location (simulation laboratory) and communicated with the process being controlled via underground long-lines. This approach, using appropriate line-driving electronics, has been highly successful even for distances of some 450 meters. Cable communication is available at Lewis between the computer facility location and the 10- by 10-Foot Supersonic Wind Tunnel and the four altitude tanks. Since programs planned for the near future involve only these experimental facilities, the central location approach will be in effect for some time. Such an approach permits double duty for the facility, with simulation evaluation of controls taking place on one shift and experimental evaluation taking place on another shift.

In the following section, some of the results obtained in the digital propulsion control studies are discussed.

DIGITAL PROPULSION CONTROL RESULTS

Digital Inlet Control

The Digital Computer Propulsion Control Facility was first used for direct digital control of an experimental mixed-compression inlet in the 10- by 10-Foot Supersonic Wind Tunnel. The function of the controls research was to evaluate shock-position control techniques as well as restart control concepts. A complete description of the test program and its results is contained in reference 2. A brief summary of the results is included in this paper.

The inlet was equipped with a translating centerbody and high-response overboard bypass doors as the control inputs. The shock-position controller was configured as

shown in the block diagram of figure 4. The purpose of the control design was to minimize shock motion caused by downstream airflow disturbances. Thus, it was to function as a shock-position regulator. Classical control design techniques (root locus analysis) were used to arrive at an acceptable inlet-shock-position-regulator control law. The continuous control law arrived at was integral in nature, with some additional lead-lag compensation. The integral control law was first implemented with electronic analog computer components, and experimental frequency response performance was obtained.

Figure 5 shows the open- and closed-loop frequency response of the normalized amplitude ratio of inlet shock position (as measured by a static pressure downstream of the throat) to an airflow disturbance as a function of the frequency of the downstream disturbance. (For brevity, only the amplitude responses are shown.) The solid curve is the open-loop or uncontrolled amplitude characteristic. The amplitude ratio of the shock motion to a downstream airflow disturbance for this and all future frequency response curves has been normalized to the steady-state, open-loop amplitude ratio. As shown in figure 5, the amplitude ratio responds about 1:1 to about 5 hertz. Beyond this, it starts to attenuate but does display a resonance at 50 to 60 hertz. The closed-loop performance of the continuous integral controller is shown by the dashed curve of figure 5. Low-frequency shock motion is greatly attenuated by the integral control action. Thus, low-frequency downstream airflow disturbances have little effect on shock position. The various system phase lags, however, cause the control action to quit at about 5 hertz. In fact, with the gain selected, the controller actually amplifies shock motion above that of the open-loop or uncontrolled case from 5 to 20 hertz. Beyond 20 hertz, response behaves as if the control had no effect. Assuming most large-magnitude airflow disturbances to be low frequency in nature, this control behavior is acceptable.

In order to evaluate the effects of using the digital computer system for direct control, the integral-shock-regulator control law was converted to a discrete-time equivalent by using Z-transform techniques. The resulting algorithm was programmed into the digital computer control system, and the experimental closed-loop results of figure 6 were obtained. Two different sample rates or control update intervals (1000 samples/sec and 100 samples/sec) were evaluated. The results as shown in figure 6 were not too different from those of the continuous controller, but some slight degradation in response did occur when using only 100 samples per second.

In the future, the advantages of having a digital computer within the control loop may lead to the use of adaptive control techniques. Here the control algorithms may be such that controls gains will be determined on line as the process varies, and the complexity of the control gain computation will become of importance. Therefore, the performance of a simple finite difference approximation (backward difference method of ref. 2) to the continuous control law was compared with the performance of the more complicated Z-transform algorithm. A frequency response comparison as shown in

figure 7 was made at the slower rate of 100 samples per second. Some degradation does occur with the backward difference approximation, but performance is still tolerable.

Digital Inlet Control (Modern Control)

During the test program just described, efforts were made to study the merits of modern or optimal control theory when applied to the shock-position-regulator problem. This study and the experimental results obtained therein are described in detail in reference 3. A brief summary of the approach taken, as well as some selected results, is contained in this paper.

The design of the shock regulator was begun with the selection of a quadratic performance index which minimized the expected frequency of inlet unstarts created by a random downstream (compressor face) airflow disturbance. The spectral density of this disturbance assumed the majority of the energy to be at low frequencies. A noisy measurement of the sensed shock position was also assumed. The controller structure, therefore, had the optimal regulator - state estimator configuration described by the block diagram of figure 8. The problem was formulated as a continuous controller, and thus a discrete equivalent had to be generated for use with the digital computer controller. The technique by which this was done is discussed in detail in an appendix to reference 3 and is not repeated herein.

The block diagram of figure 9 shows the various elements which comprise the digital computer implementation of the modern or optimal shock-position regulator. The discrete optimal regulator - state algorithm did not permit the system to be sampled less frequently than 1000 samples per second. The sampled-data system became unstable if sampling less than once every 1 millisecond was attempted.

Figure 10 compares the closed-loop frequency response performance for the discrete optimal control with the continuous version implemented with analog computer components. The curves show the normalized amplitude ratio of shock position to the disturbance airflow against frequency. As shown in figure 10, there is very little difference between the analog and digital control performance. The curves show that the low-frequency shock motion is attenuated, which is similar to the integral control action of the classical inlet control design. The optimal regulator has been forced to this type of response by the nature of the spectral density of the disturbance (most of the energy at the low frequencies).

It should be emphasized at this point that the frequency response results of figure 10 are included only to show that a complicated, continuous, optimal regulator - state estimator control law could be discretized for use in a digital computer sampled-data system. The exact discretization demanded the 1000-sample-per-second rate. No effort

was made to develop control law simplifications which would reduce the required sampling rates.

Digital Turbojet Engine Control

The capabilities of digital computers for turbojet engine control were investigated with a J85-GE-13 engine in a Lewis sea-level test stand. The computer system was programmed to implement the continuous bill-of-material control laws in a discrete fashion. Figure 11 compares the time responses of several engine variables for a throttle step from idle to military using the continuous intact hydromechanical controller with those using the discrete digital computer control. Although only an update interval of 2 milliseconds (500 samples/sec) is shown in the figure, identical transient performance was obtained at update intervals to 25 milliseconds (40 samples/sec). Beyond 25 milliseconds, the speed response began to become oscillatory. In figure 11 it can be seen that the digital control (solid curves) responds slightly faster than the hydromechanical controller (dashed curves). This slight difference was determined to be due to some small differences between the nominal control schedules programmed in the computer and the actual cam schedules in the specific hydromechanical controller used.

Using the Lewis digital system, the controller could sample measured control variables, compute the control algorithm using these sampled measurements, and output commands in an elapsed time of about 1.4 milliseconds (1400 μsec). The sequence of operations is diagramed in figure 12. The sequence was initialized with a priority interrupt from an interval timer. As shown in the figure, the total control computation takes approximately 1.408 milliseconds (1408 μsec). If the system is updating every 2 milliseconds (2000 μsec), there will be 0.6 millisecond (600 μsec) of idle time available between interrupts. At a 25-millisecond update interval though, the computer would be busy only 6 percent of the time. This "spare time" might be necessary if the computer would also be required to compute a complicated inlet control law and to update the inlet every 5 milliseconds or so.

Looking ahead then, to the time when the computer might be asked to do many more on-line, real-time tasks other than inlet and engine control, methods for reliably extending control update intervals were investigated. The curves of figure 13 show some of the results of this investigation. A prediction algorithm was selected and applied to the sampled measurements. This technique permitted engine transient performance at 150-millisecond updates to closely match the 2-millisecond performance without prediction. Essentially, the prediction algorithm uses the present measurement and past measurements to determine the trend or direction in which particular measured variables are headed. It can then predict what the variable might be at some time during the

interval. It then uses the predicted value at some selected instant within the interval to compute the controller inputs to the engine. The complete details of this engine digital controls research activity are documented in reference 4. Also included is a complete description of the experimental equipment needed to accomplish electronic engine control.

Fail-Operational Digital Engine Control

A digital engine control study was carried out in the sea-level test stand to utilize the extensive computational and decision making potential of the digital computer to perform new control functions not attainable with state-of-the-art hydromechanical controllers. The concept studied was termed fail-operational control. Its purpose was to develop a controller able (1) to detect failures in certain specific sensed engine measurements, (2) to adapt to these failures, and (3) to continue to provide engine operation with as little performance degradation as possible.

In this first attempt at implementing a fail-operational control, only the sensed measurements of engine rotor speed and compressor-discharge static pressure were considered as candidates for possible failure. These are two primary measurements used in the J85-GE-13 bill-of-material control law. The fail-operational system was designed to operate with either or both of the two sensors failed. This investigation is described in reference 5. A brief description of the system and the experimental results obtained using it are contained in the next few paragraphs.

The basis of the fail-operational control is the fact that the compressor-discharge static pressure p_3 and engine rotor speed N are very strongly dependent on one another because of the inherent cycle characteristics of the turbojet engine. Figure 14 is a plot of this relation during normal steady-state operation as well as during accelerations and decelerations. The data are for speeds from idle to military (full 100 percent speed) and were taken at sea-level static conditions. The computer was programmed to store a representation of this characteristic in memory for use during a fail-operational control condition.

A generalized block diagram of the fail-operational control is presented in figure 15. The sensor measurements of engine rotor speed N and compressor-discharge static pressure p_3 are brought into the computer controller through its normal sampling mechanism. Before the sampled measurement is used in the normal engine control algorithm, however, a failure-detection algorithm is applied to each. If a failed sensor is detected, for pressure p_3 for instance, the control logic will switch from the incorrect measured value of p_3 to a stored value of p_3 representative of compressor-discharge exit static pressure at the speed at which the engine is operating. The normal engine

control algorithm will then be exercised, using the unfailed speed measurement and the modeled p_3 pressure value. The control will also use the throttle-input and compressor-face temperature and pressure measurements.

As shown in figure 14, the speed-pressure characteristic is double and even triple valued at the high end. This characteristic is due to exhaust nozzle motion caused by the turbine-discharge-temperature override control loop, which is standard on the J85-GE-13 engine. In order to avoid this multivalued condition and to be able to put realizable characteristic functions into the computer memory, the normal bill-of-material control was modified slightly. A limit was imposed on the minimum allowable exhaust nozzle area such that the temperature override would not be activated. Also, a limit was placed on the maximum throttle position that the control would accept. Admittedly, these limits sacrificed some thrust capability, but they did permit a straightforward approach to computer modeling and storage of the engine speed-pressure characteristic. The actual data that were tabulated in memory for use in the fail-operational control are shown on figure 16. Data of speed against pressure and pressure against speed are redundant information, but both are stored in the computer to simplify the retrieval from memory.

One of the innovations of the computer algorithms developed in this fail-operational investigation is that a self-teaching feature was developed for modeling the speed-pressure characteristics. The control was designed to start from a crude generalized engine characteristic for a J85-GE-13. Then, with all sensors operating, the control could teach itself the exact data for the engine being controlled. The system would require both a slow and a fast throttle transient to generate, in memory, data similar to those in figure 16. In this way the system operated with actual engine characteristics rather than precalculated nominal or average values for the whole family of J85-GE-13 engines. A detailed discussion of the fail-operational control is given in reference 5.

Figure 17 shows the response of the engine rotor speed for a throttle step from idle to military power setting under both normal control and fail-operational control. Cases for either a compressor pressure or engine speed sensor failure are shown. (Note that speed information for this data is obtained from speed instrumentation distinct from the control speed sensor whose failure is being simulated.) In these curves it was assumed that the individual sensor failures were detected prior to the start of the transient. Transient responses in which the individual sensor failed during the transient were also taken and operation was identical to figure 17. For either type of failure, correspondence to normal control is good. However, because throttle limits were built into the algorithm, the speed under fail-operation control does not quite reach full military speed. Likewise, the thrust response curves of figure 18 show that thrust also is limited by a small amount at either condition of fail-operational control. This limitation is due to lower speeds and the fact that the exhaust nozzle area was prevented from going fully

closed to avoid the turbine-discharge-temperature override which would modulate the area.

Simultaneous failures of both the speed and pressure sensors were accommodated in the fail-operational control. Detection of a double sensor failure put the normal engine control into a throttle-rate-limit mode. In this mode, regardless of the throttle input from the outside, the controller would schedule engine operation per a selected rate of change of throttle position until the final throttle input was achieved. Figure 19 shows the response under the double-sensor-failure condition. Speed response from idle to military is about 30 seconds. The throttle rate limit was selected conservatively to demonstrate computer control capability. No attempt was made to optimize the response under double failures.

Inlet-Engine Digital Integrated Control

The Lewis Digital Computer Propulsion Control Facility was most recently employed in the control integration of an experimental supersonic mixed-compression inlet and a TF-30/P-3 afterburning turbofan engine. This experimental program is the subject of a paper to be presented at this session by Mr. P. Batterton and therefore is not discussed herein. A detailed discussion of that work is contained in reference 6.

Present Activities

At the present time the computer facility is being employed to study digital control of advanced turbofan engines. The engines presently are simulated in real time on the Lewis hybrid computer system, and new modes of control using a digital computer are being evaluated. These are complete wide-range simulations of operation at many altitude and Mach number conditions. In conjunction with this effort, experimental programs in the altitude test facilities are being planned to verify the control concepts being studied.

CONCLUDING REMARKS

If we consider the Lewis Digital Computer Propulsion Control Facility as a tool for propulsion control mode studies regardless of the future type of hardware implementation of the control, the past 4 years have been highly successful. The ability to assess control concepts and then simply modify software to investigate other control approaches has greatly expedited our research activities.

If we consider the digital facility as a predecessor of the type of control hardware that will actually be available for future operational propulsion systems, much valuable information has been learned. First, a modern digital control computer operating as a sampled-data system can definitely perform the control task for a complete supersonic airbreathing propulsion system. Modern computers are certainly fast enough and, equipped with sufficient memory capacity, can perform tasks previously considered impracticable.

Much more work remains to be done to ensure that new digital control laws can be reliably executed under the ever-changing requirements and conditions that a propulsion system encounters in an operational flight application. Some of these potential problems can, with careful planning, be attacked in ground test facilities and with sophisticated simulations. The utilization of the Lewis Digital Computer Propulsion Control Facility is directed toward this end. Other problems will have to be solved with flight programs such as the F-111 IPCS and YF-12 cooperative control activities.

REFERENCES

1. Arpasi, Dale J.; Zeller, John R.; and Batterton, Peter G.: A General Purpose Digital System for On-Line Control of Airbreathing Propulsion Systems. NASA TM X-2168, 1971.

2. Neiner, George H.; Cole, Gary L.; and Arpasi, Dale J.: Digital-Computer Normal-Shock-Position and Restart Control of a Mach 2.5 Axisymmetric Mixed-Compression Inlet. NASA TN D-6880, 1972.

3. Zeller, John R.; Lehtinen, Bruce; Geyser, Lucille C.; and Batterton, Peter G.: Analytical and Experimental Performance of Optimal Controller Design for a Supersonic Inlet. NASA TN D-7188, 1973.

4. Arpasi, Dale J.; Cwynar, David S.; and Wallhagen, Robert E.: Sea-level Evaluation of Digitally Implemented Turbojet Engine Control Functions. NASA TN D-6936, 1972.

5. Wallhagen, Robert E.; and Arpasi, Dale J.: A Self-Teaching Digital-Computer Program for Fail-Operational Control of a Turbojet Engine in a Sea-Level Test Stand. NASA TM X-3043, 1974.

6. Batterton, Peter G.; Arpasi, Dale J.; and Baumbick, Robert J.: Digital Integrated Control of a Mach 2.5 Mixed-Compression Supersonic Inlet and an Augmented Mixed-Flow Turbofan Engine. NASA TM X-3075, 1974.

TABLE I. - SIGNAL PROCESSING CAPABILITY

	Present complement	Fully expanded
Signal inputs from propulsion system	100	100
Signal outputs to propulsion system	54	54
Analog-to-digital conversion channels	64	64
Period-to-digital conversion channels	10	20
Logical outputs	64	64
Digital-to-analog conversion channels	26	42
External priority interrupt	10	22

TABLE II. - FACILITY SPECIFICATIONS

Digital computer	
Magnetic core memory size, words	16 384
Word length, bits plus parity	16
Memory cycle time, nsec	750
Add time, μsec	1.5
Subtract time, μsec	1.5
Multiply time, μsec	4.5
Divide time, μsec	8.25
Load time, μsec	1.5
Store time, μsec	1.5
Indirect addressing	Infinite
Indexing	Total memory
Priority interrupts	28 Separate levels
Index registers:	
Independent	1
In conjunction with lower accumulator	1
Physical size, cm (in.):	
Width	60.9 (24)
Height	157.4 (62)
Depth	76.2 (30)
Interval timers	
Complement	2
Accuracy, clock pulses	±1
Clock rates, kHz	572, 286, 160, 143, 80, 71.5, 40, 35.75, 20, 10
Counter	16-Bit binary
Output	Priority interrupt to computer
Analog acquisition unit	
Number of multiplexers, digitizers, and sample and holds	2
Overall sample rate (maximum), kHz	40
Resolution of digital data, bits	12 (plus sign)
Output code	Two's complement
Number of channels	64
Input range, V (full scale)	±10
Input impedance, MΩ (shunted by 10 pF)	10
Maximum source resistance, Ω	1000
Conversion time, μsec	38
Input settling time, μsec	9
Sample-and-hold aperture time, nsec	500
Safe input voltages, V	±20 sustained ±100 for less than 100 μsec
Total error with calibration, percent	0.073

TABLE II. - Concluded. FACILITY SPECIFICATIONS

Frequency acquisition unit	
Number of channels	10
Nature of input	Continuously varying or pulsatile
Resolution of digital data, bits	12
Switch selectable clock rates, kHz	20, 80, 100, 400, external
Overall accuracy, bits	±1
Update rate	Once per cycle of input frequency
Maximum input frequency, kHz	1
Input amplitude range	100 mV to 30 V peak to peak
Analog output unit	
Total number of digital-to-analog conversion channels	26
Resolution (10 channels), bits	12 (plus sign)
Resolution (16 channels), bits	11 (plus sign)
Output voltage range, V full scale	±10
Output current (maximum), mA	10
Output impedance, Ω	<1
Accuracy (12 bit), percent of full scale	±0.1
Accuracy (13 bit), percent of full scale	±0.05
Slew rate, V/μsec	1
Settling time for 10-V step to within 0.05 percent of final value, μsec	20
Logical output unit	
Number of electronic switch outputs	32
Number of contact closure outputs	32
Maximum voltage, V	30
Maximum current, mA	100
Priority interrupt processor	
Number of channels	10
Input impedance, kΩ	47
Input voltage range, V	±10
Comparator switching	Trigger on rise or fall
Comparator hysteresis	Adjustable from 35 mV to 650 mV
Comparator output, V	+7
Monostable multivibrator:	
Pulse width, μsec	3
Pulse height, V	+7

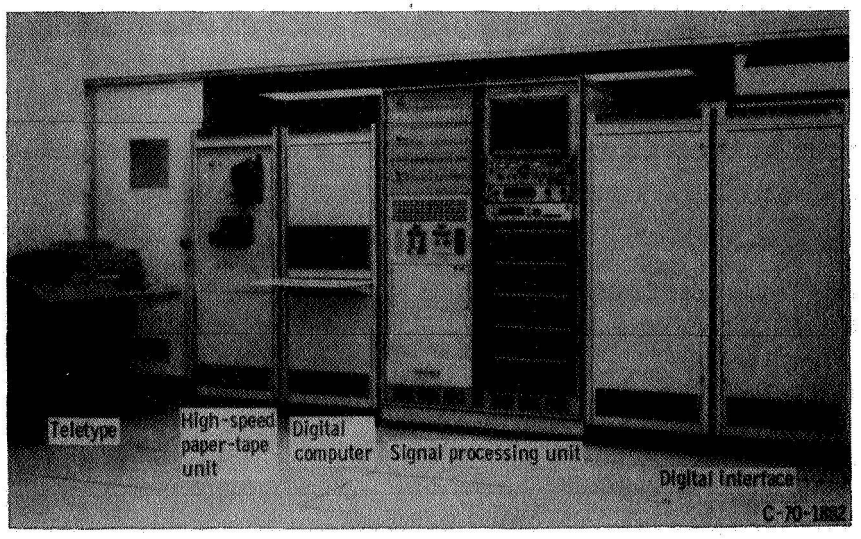

Figure 1. - Digital computer propulsion control facility.

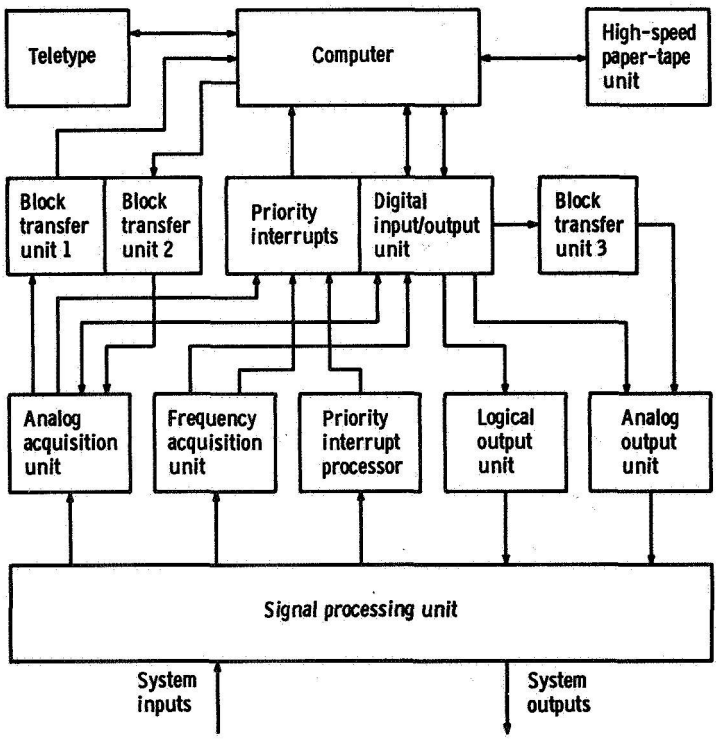

Figure 2. - Block diagram of digital control facility.

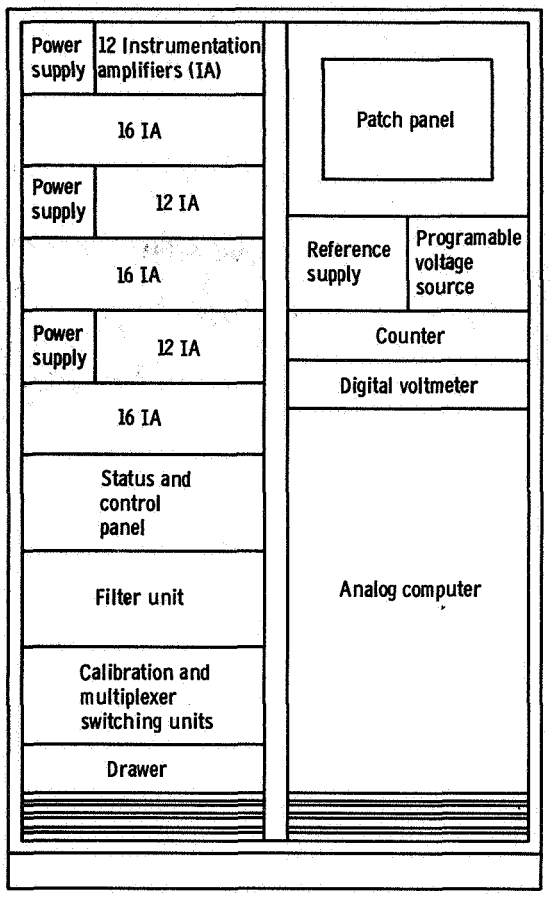

Figure 3. - Cabinet layout of signal processing unit.

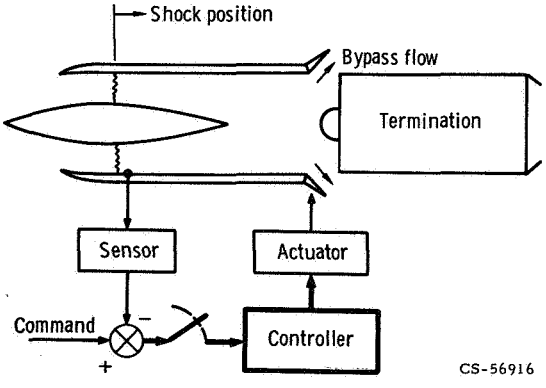

Figure 4. - Block diagram of shock position control system.

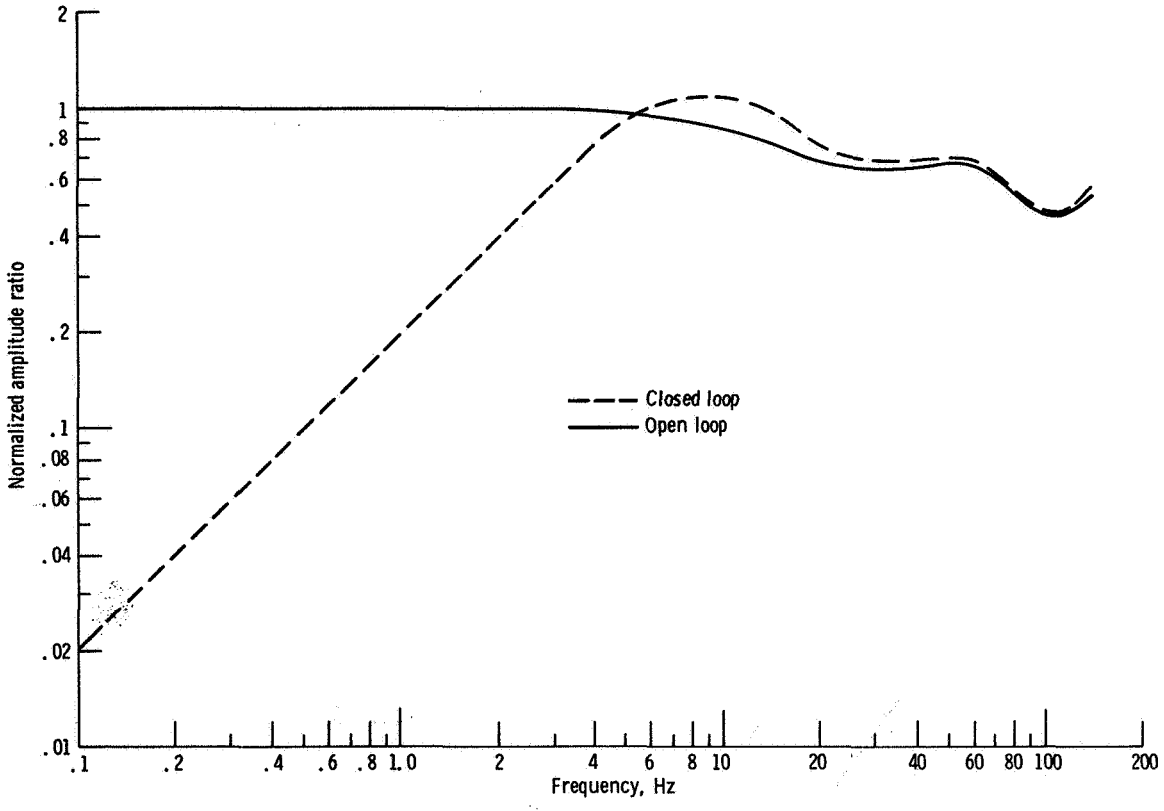

Figure 5. - Comparison of experimental open-loop and closed-loop frequency response of normalized amplitude ratio of shock position to airflow disturbance.

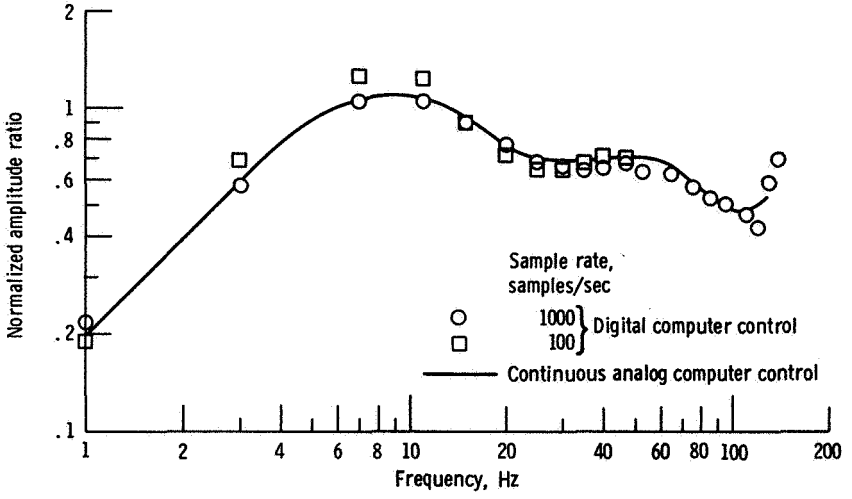

Figure 6. - Comparison of experimental closed-loop frequency response performance using analog computer control and z-transform digital computer control at two different sampling rates.

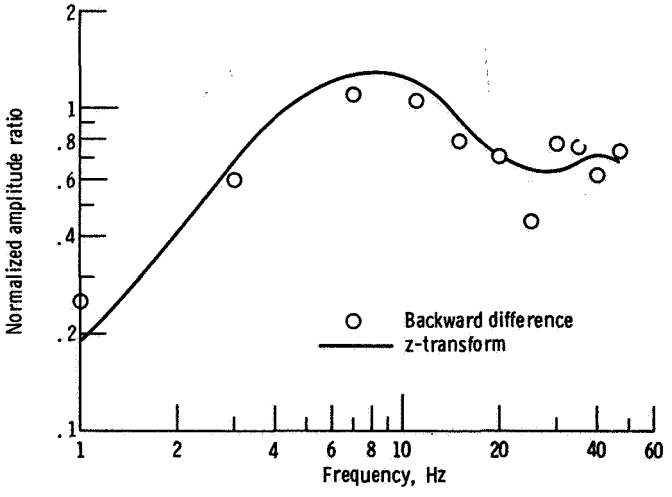

Figure 7. - Comparison of experimental closed-loop frequency response for z-transform and backward difference digital computer algorithms using sample rate of 100 samples per second.

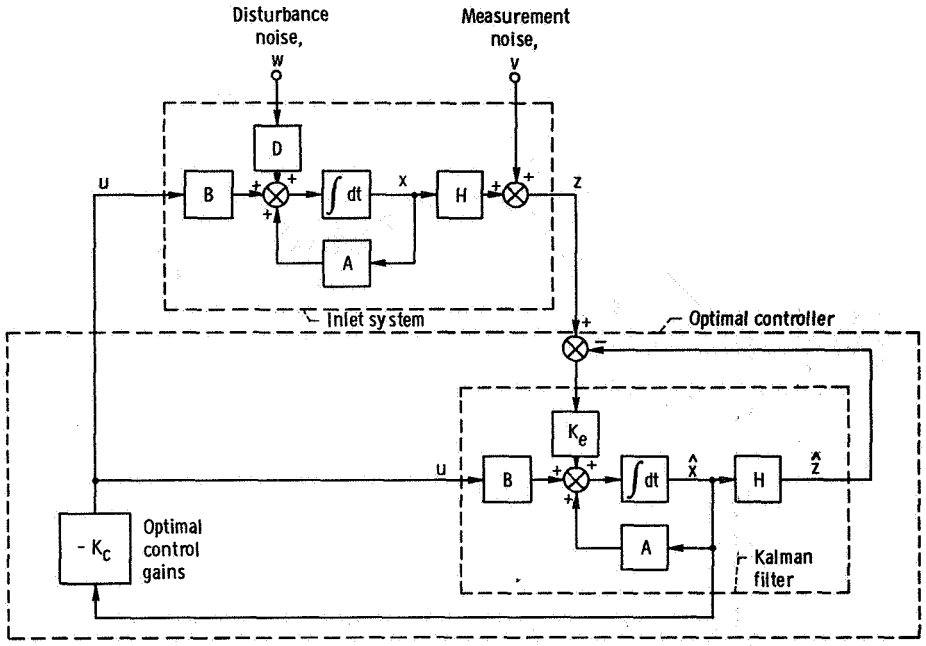

Figure 8. - Block diagram of combined optimal regulator - state estimator. (Symbols used are conventional modern/optimal control notation.)

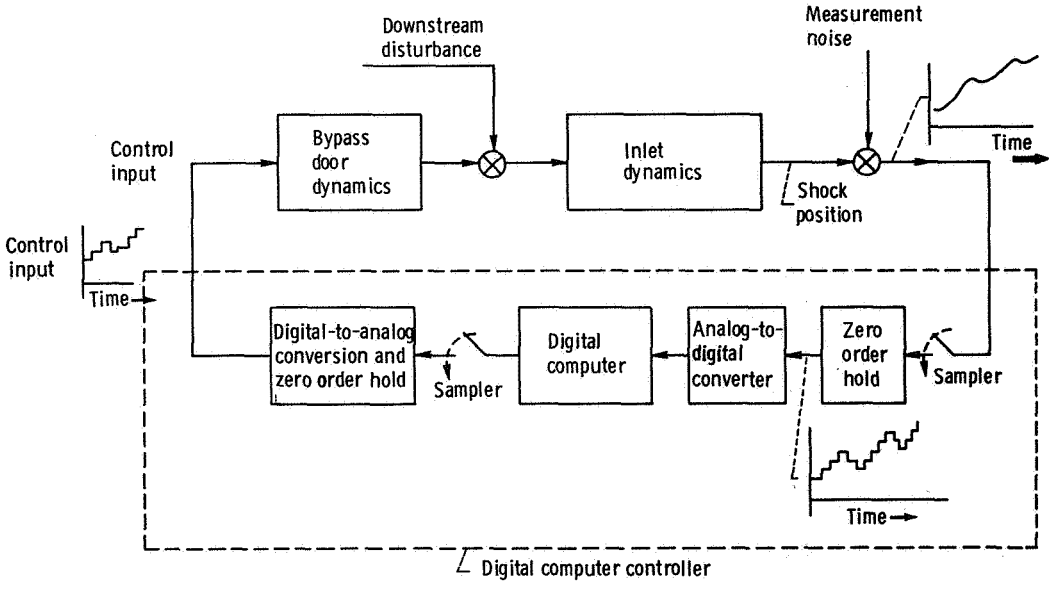

Figure 9. - Block diagram of digital computer inlet control system.

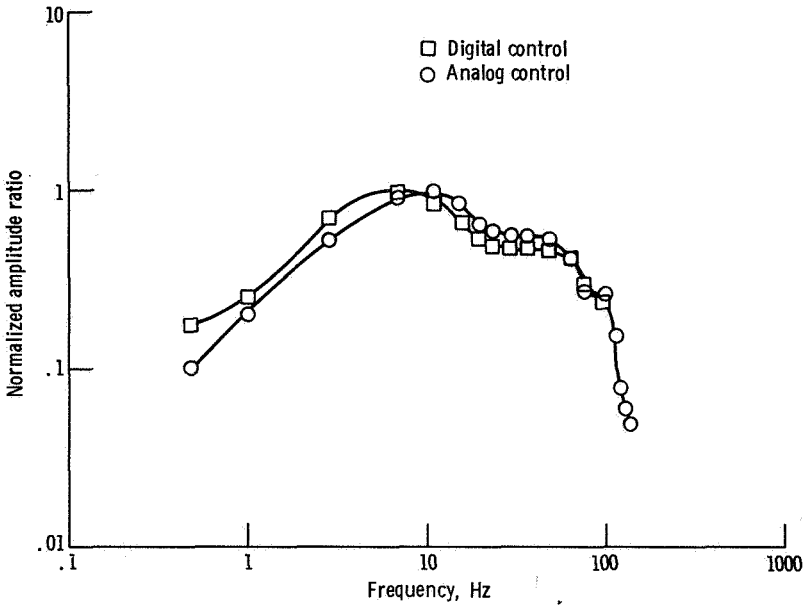

Figure 10. - Comparison of closed-loop experimental frequency responses of shock position to disturbance airflow amplitude ratio using analog and digital computer implementations of optimal regulator - state estimator control law.

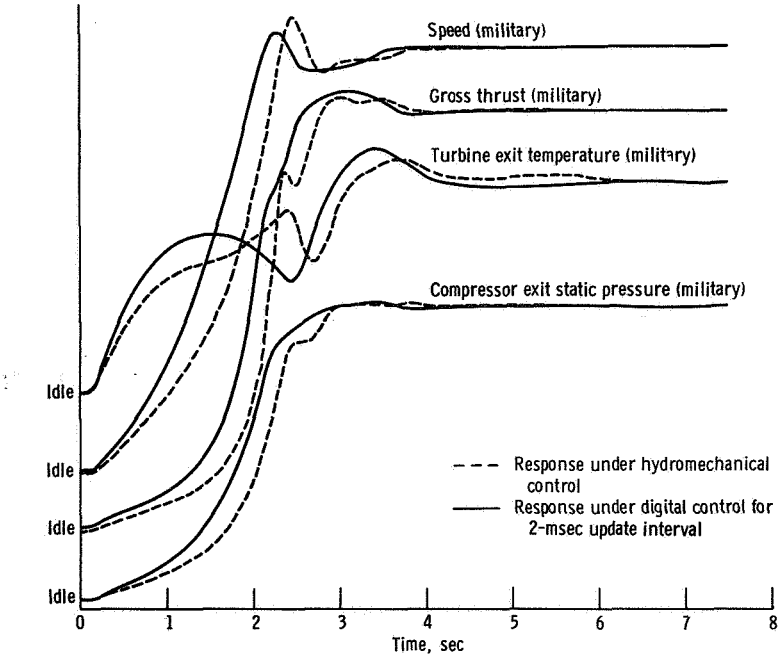

Figure 11. - Comparison of digital and hydromechanical controls for throttle step from idle to military.

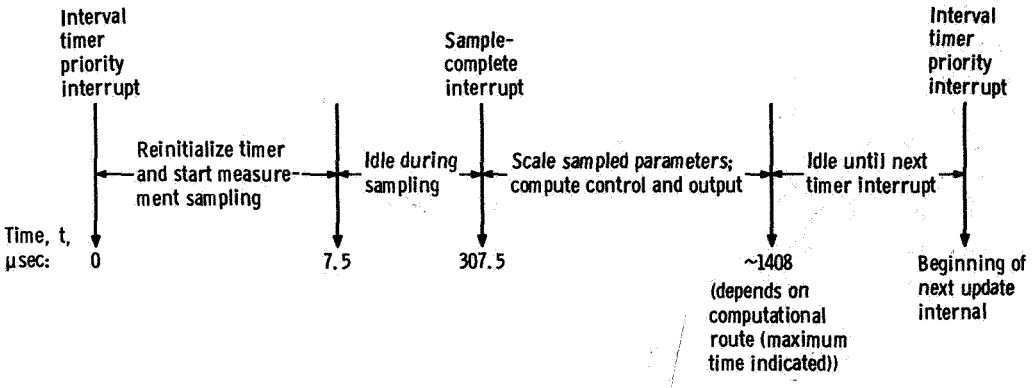

Figure 12. - Timing diagram for typical update interval.

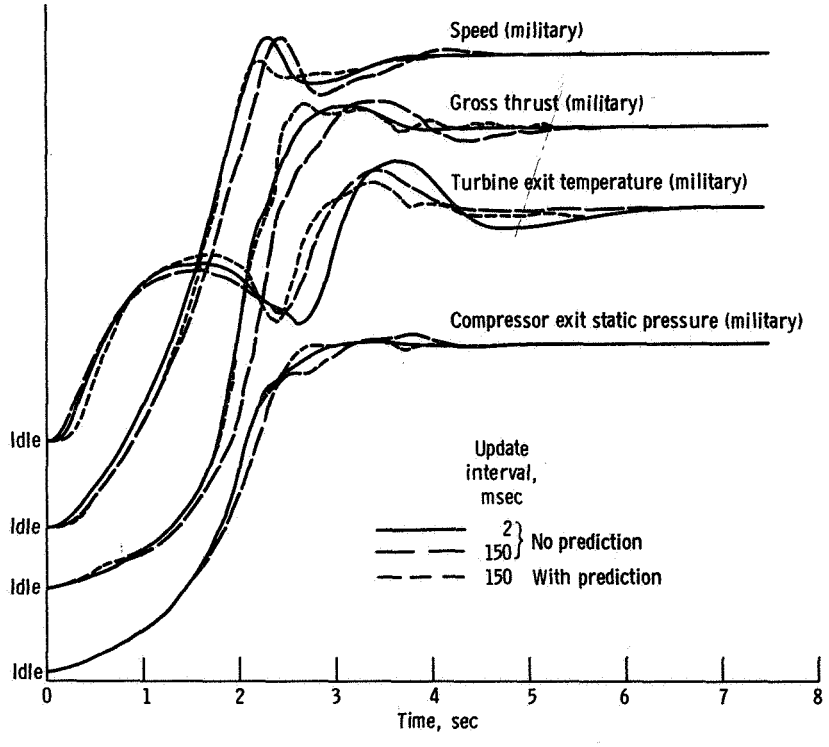

Figure 13. - Effects of prediction on engine response for throttle step from idle to military.

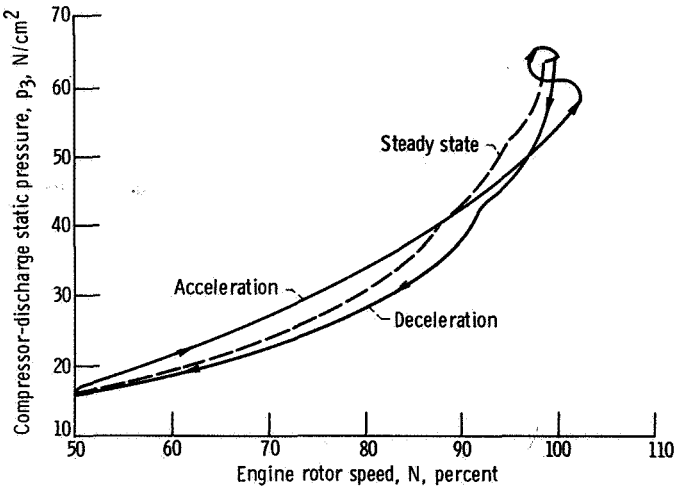

Figure 14. - Compressor-discharge static pressure as function of engine rotor speed for normal digital control.

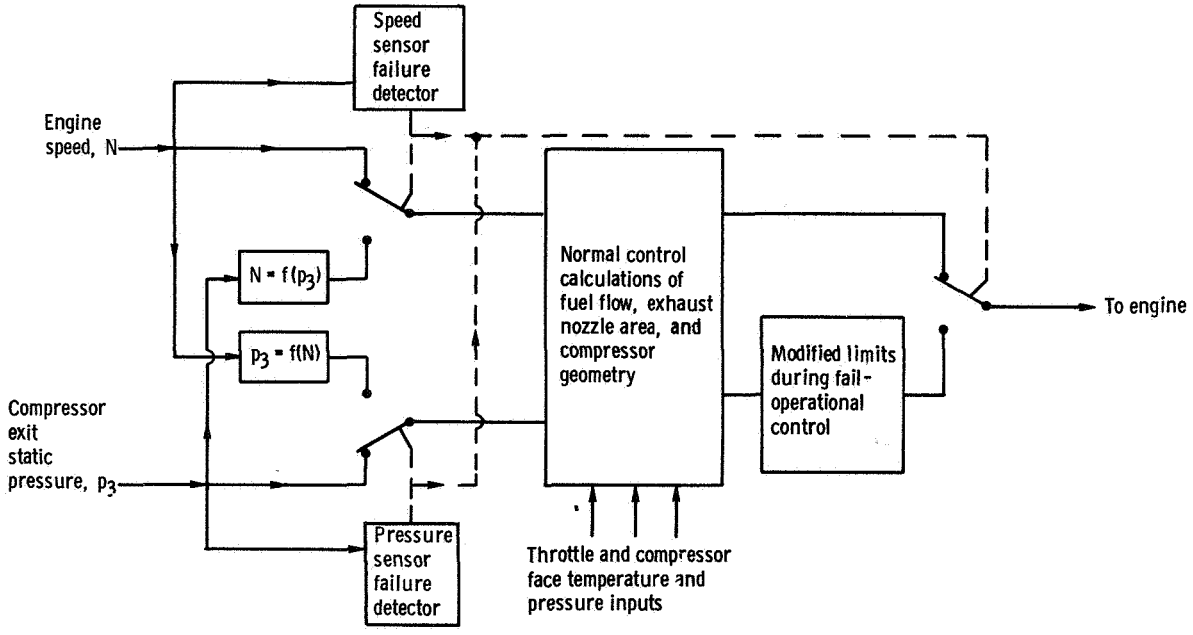

Figure 15. - Block diagram of fail-operational control.

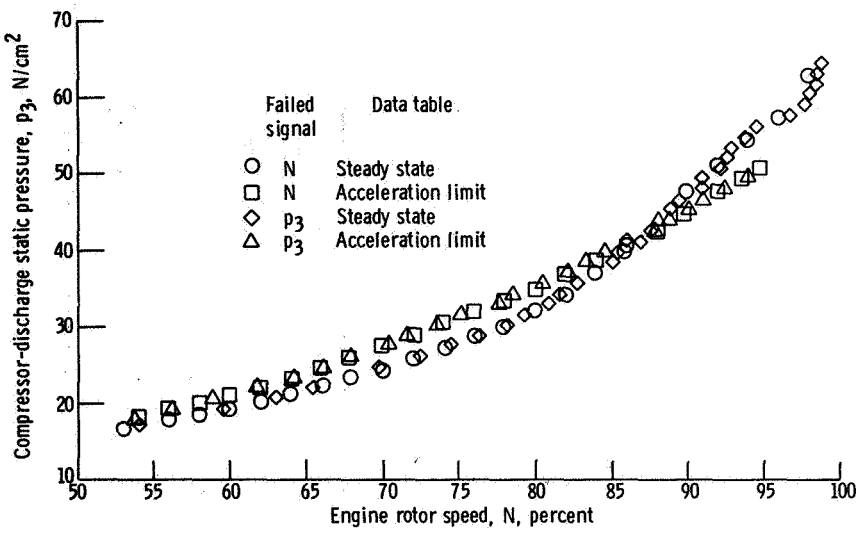

Figure 16. - Plot of tabulated values of compressor-discharge static pressure and engine rotor speed as functions of each other for fail-operational control programs.

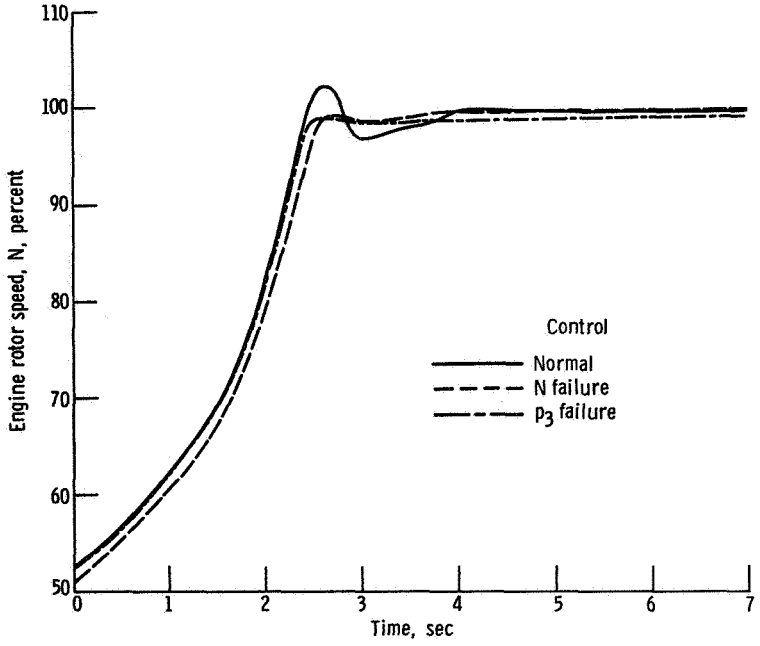

Figure 17. - Step responses of engine rotor speed from idle to 100 percent rotor speed for normal digital control and engine rotor speed and compressor-discharge static pressure p_3 fail-operational controls.

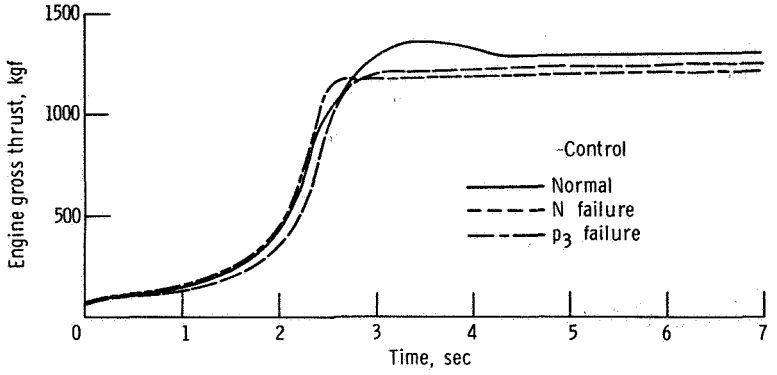

Figure 18. - Step responses of engine gross thrust from idle to 100 percent rotor speed for normal digital control and engine rotor speed N and compressor-discharge static pressure p_3 fail-operation controls.

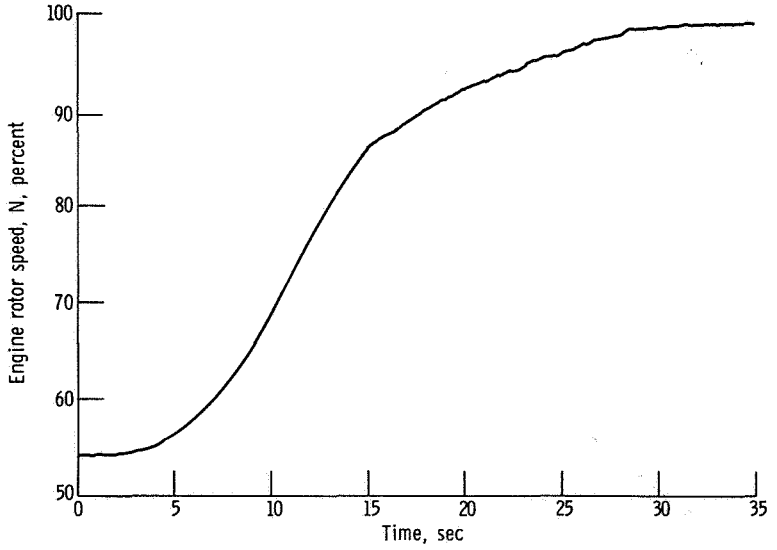

Figure 19. - Step response of engine rotor speed from idle to 100 percent rotor speed for combined engine rotor speed N and compressor-discharge static pressure p_3 fail-operational control.